AD-A081 657 SOUTHWEST RESEARCH INST SAN ANTONIO TEX F/G 11/2
COMPRESSIVE STRENGTH AND DAMAGE MECHANISMS IN CERAMIC MATERIALS--ETC(U)
FEB 80 J LANKFORD N00014-75-C-0668
UNCLASSIFIED NL

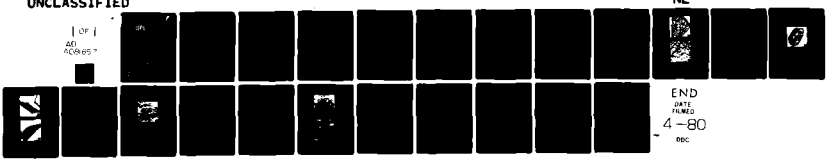

END
DATE FILMED
4-80
DDC

COMPRESSIVE STRENGTH AND DAMAGE MECHANISMS IN CERAMIC MATERIALS.

LEVEL II

BY

JAMES LANKFORD

INTERIM TECHNICAL REPORT. 1 Jul 79 - 31 Jan 80

ONR CONTRACT No. N00014-75-C-0668
ONR CONTRACT AUTHORITY NR 032-553/1-3-75(471)
SwRI PROJECT No. 02-4231

FOR

OFFICE OF NAVAL RESEARCH
ARLINGTON, VA 22217

BY

SOUTHWEST RESEARCH INSTITUTE
SAN ANTONIO, TEXAS

FEB 1980

SOUTHWEST RESEARCH INSTITUTE
SAN ANTONIO HOUSTON

SECURITY CLASSIFICATION OF THIS PAGE *(When Data Entered)*

REPORT DOCUMENTATION PAGE		READ INSTRUCTIONS BEFORE COMPLETING FORM
1. REPORT NUMBER	2. GOVT ACCESSION NO.	3. RECIPIENT'S CATALOG NUMBER
4. TITLE *(and Subtitle)* Compressive Strength and Damage Mechanisms in Ceramic Materials		5. TYPE OF REPORT & PERIOD COVERED Interim Technical Report 1 July 1979 - 31 January 1980
		6. PERFORMING ORG. REPORT NUMBER
7. AUTHOR(s) James Lankford		8. CONTRACT OR GRANT NUMBER(s) N00014-75-C-0668
9. PERFORMING ORGANIZATION NAME AND ADDRESS Southwest Research Institute 6220 Culebra Road (P. O. Drawer 28510) San Antonio, TX 78284		10. PROGRAM ELEMENT, PROJECT, TASK AREA & WORK UNIT NUMBERS NR 032-553/1-3-75(471)
11. CONTROLLING OFFICE NAME AND ADDRESS Office of Naval Research 800 North Quincy Arlington, VA 22217		12. REPORT DATE 15 February 1980
		13. NUMBER OF PAGES
14. MONITORING AGENCY NAME & ADDRESS *(if different from Controlling Office)*		15. SECURITY CLASS. *(of this report)* Unclassified
		15a. DECLASSIFICATION/DOWNGRADING SCHEDULE

16. DISTRIBUTION STATEMENT *(of this Report)*

17. DISTRIBUTION STATEMENT *(of the abstract entered in Block 20, if different from Report)*

18. SUPPLEMENTARY NOTES

19. KEY WORDS *(Continue on reverse side if necessary and identify by block number)*

Compressive Strength	Microcrack Initiation	Aluminum Oxide
Temperature Effects	Ceramics	Cracking Threshold
Loading Rate	Silicon Carbide	Fractography
	Silicon Nitride	Fracture Mechanism

20. ABSTRACT *(Continue on reverse side if necessary and identify by block number)*

Compressive strength measurements as a function of temperature and loading rate, and microhardness measurements as a function of temperature, have been carried out for Al_2O_3, SiC, and Si_3N_4. Results are correlated in terms of current theories connecting compressive strength, hardness, fracture toughness, and indentation microfracture. It is found that while high loading rates can suppress high temperature intergranular compressive fracture in SiC, this is not true in Al_2O_3. The threshold crack size for indentation

DD FORM 1 JAN 73 1473

SECURITY CLASSIFICATION OF THIS PAGE *(When Data Entered)*

microfracture as a function of temperature seems to correlate at least as well (if not better) with compressive strength as with hardness, and temperature-controlled compressive fracture mechanisms seem to operate during indentation fracture at corresponding temperatures.

TABLE OF CONTENTS

LIST OF FIGURES

ABSTRACT

Compressive strength measurements as a function of temperature and loading rate, and microhardness measurements as a function of temperature, have been carried out for Al_2O_3, SiC, and Si_3N_4. Results are correlated in terms of current theories connecting compressive strength, hardness, fracture toughness, and indentation microfracture. It is found that while high loading rates can suppress high temperature intergranular compressive fracture in SiC, this is not true in Al_2O_3. The threshold crack size for indentation microfracture as a function of temperature seems to correlate at least as well (if not better) with compressive strength as with hardness, and temperature-controlled compressive fracture mechanisms seem to operate during indentation fracture at corresponding temperatures.

I. Introduction

In order to gain insight into the mechanisms responsible for solid particle impact damage in engineering ceramics, a program of research has been carried out which is aimed at understanding compressive damage in these materials. High compressive stresses are generated during impact (indentation) loading, and it is thought that compressive failure micromechanisms are involved in the associated cracking process. Moreover, compressive strength is directly related to material hardness,[1] which together with fracture toughness is thought[2,3] to control indentation crack size and corresponding load level.

The results described in this report represent approximately the most recent seven-month period of an ongoing program. Findings are presented and analyzed in the context of earlier data[4-6] obtained for identical materials tested under different loading rate/temperature conditions.

II. Experimental Approach

Compressive strength tests were carried out over a range of temperatures (23°-1600°C) within a special Hopkinson pressure bar system,[4,6] whereby strain rates of $\dot{\varepsilon} = 10^3 s^{-1}$ were achieved. These are extremely difficult tests to run, requiring great precision in specimen preparation and alignment in order to ensure valid compressive strength measurements. Specimens of Al_2O_3, SiC, and Si_3N_4, whose material properties are listed in Table I, were compressed using sintered α-SiC

TABLE I

NOMINAL AMBIENT MATERIAL PROPERTIES

Material	Manufacturer/Designation	Tensile Strength (MN/m^2)	DPH (kg/mm^2)	K_c ($MNm^{-3/2}$)	Grain Size (μm)
SiC	Carborundum/Sintered α-SiC	345	2800	4.4	3-5
Si_3N_4	Norton/NC-132	810	1860	4.8	0.5-3
Al_2O_3	General Electric/Lucalox	215	2230	4.0	20-30

platens (for high temperature strength) separated from the ultra high strength steel loading rods by a second set of AD 999 alumina platens (to minimize heat flow into the loading rods). To the knowledge of the writer, these tests represent the combined highest temperatures and strongest materials, by far, ever tested under such high strain rate, controlled load conditions. Following each test, scanning electron microscope fractographic examination was carried out on the resulting fragments.

Concurrently, elevated temperature microhardness tests were performed for all three materials, specimen temperatures ranging from 23° to 1000°C, over a range in indentation loads from 2-800 gms. Tests were performed under an argon environment in a modified Tukon microhardness tester, with the duration of indentation-specimen contact being one second. Hardness values were taken as the average of at least three drops each at 200, 400, 600, and 800 gms. Tests at temperatures in excess of 1000°C were precluded due to cracking in the diamond mounting.

Following these tests, specimens were examined in the SEM. Threshold indentation crack sizes were measured, and lateral and radial microcrack mechanisms were analyzed.

III. Results

A. Compression Tests

The high loading rate compressive strength results are plotted as a function of temperature as shown in Figure 1 for Al_2O_3. Also plotted are results of tests carried out at lower loading rates.

Figure 1 represents the now complete mapping of compressive strength (σ_c) for Al_2O_3 as a function of temperature (T) and strain rate ($\dot{\varepsilon}$) from $-200 \leq T \leq 1600°C$, $7 \times 10^{-5} \leq \dot{\varepsilon} \leq 2 \times 10^{3} s^{-1}$ (also shown is the tensile strength (σ_T) and the threshold stress for compressive damage, σ_{AE}). The intermediate temperature (200-400°C) transition region, previously suggested[4] as controlled by twinning, is significantly reduced at $\dot{\varepsilon} = 10^{3} s^{-1}$. However, high temperatures (>600°C) still are able to lower the compressive strength to a degree more or less proportional to that experienced at the lower strain rates.

Previously it was shown[7] that for these latter rates, the high temperature compressive fracture mode was intergranular; a transitional combined intergranular-transgranular region was noted for $350 \leq T \leq 750$, with nearly total transgranular fractography found for lower temperatures. One of the objectives of the recent tests was to determine whether high loading rates could alter this picture. However, as shown in Figure 2, this clearly was not the case; even for such a high rate of deformation, failure at T = 1500°C was totally intergranular, while at T = 600°C, the fracture surface is mixed intergranular-transgranular. At lower temperatures, transgranular failure predominates.

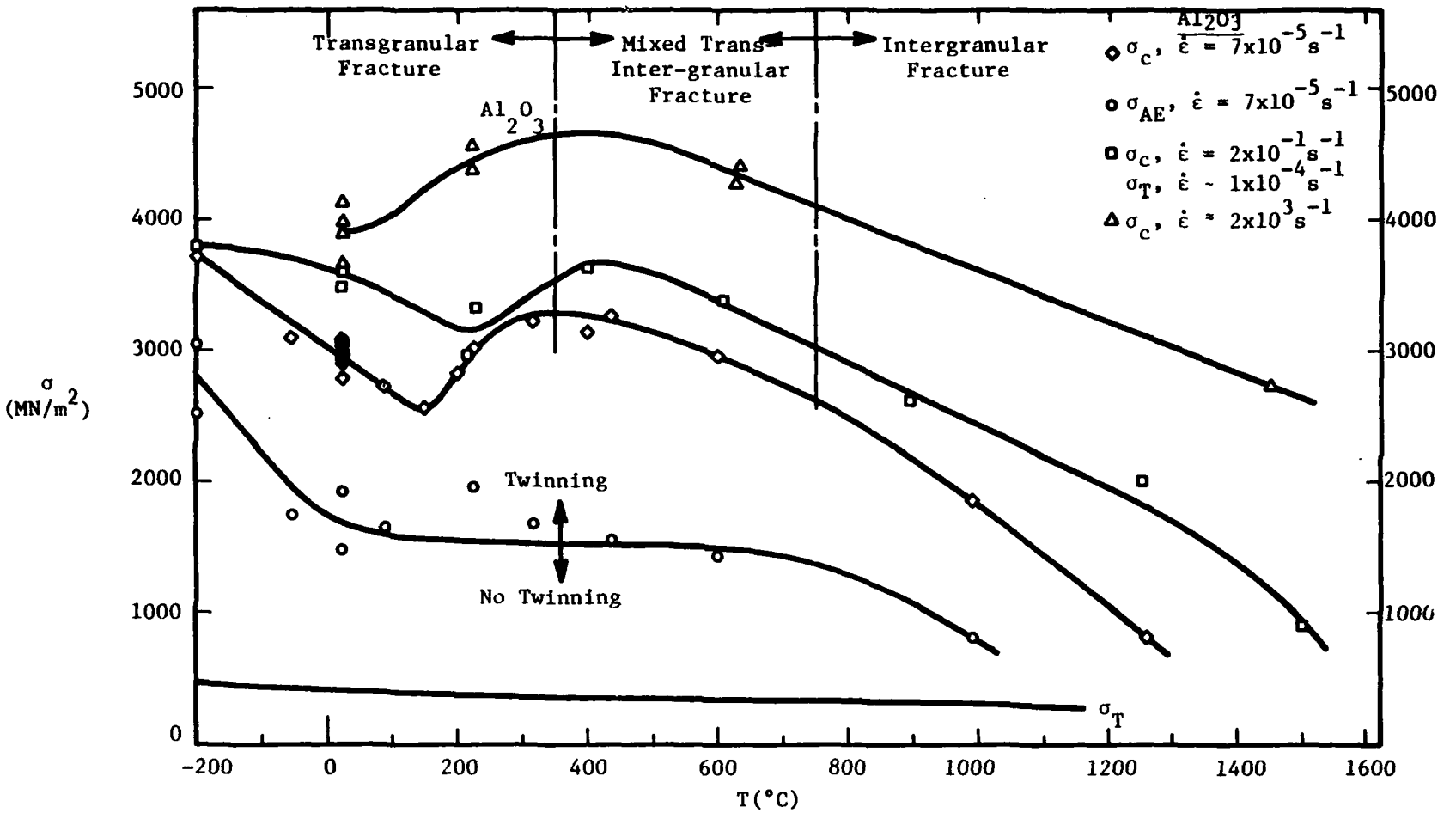

Figure 1. Al_2O_3 Strength Versus Temperature and Strain Rate.

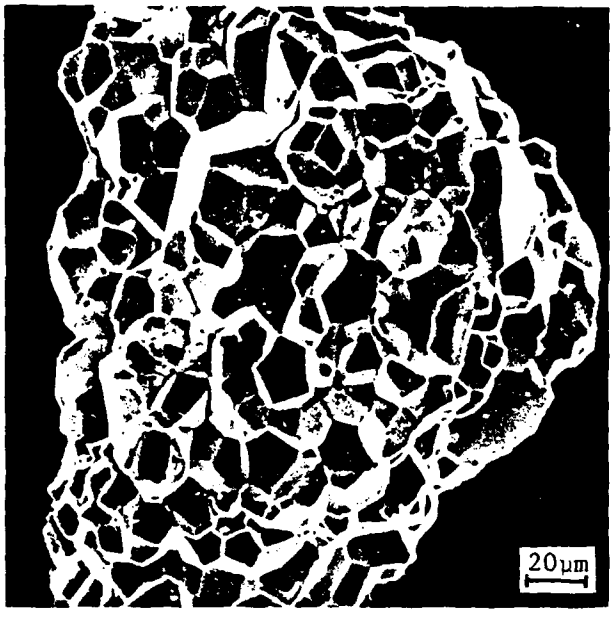

a) Intergranular Fracture, T = 1500°C

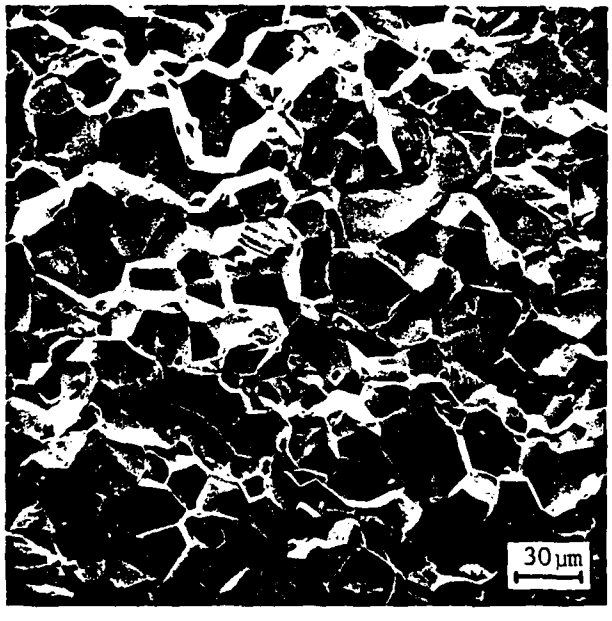

b) Intergranular-Transgranular Fracture, T = 600°C

Figure 2. Al_2O_3 Compressive Failure Fracture Surfaces, $\dot{\varepsilon} = 2 \times 10^3 s^{-1}$.

A good compressive test of a brittle material corresponds to a specimen essentially exploding via the linkup of inumerable microcracks, reducing itself to a pile of dust (plus a few larger fragments, as in Figure 2). Normally, this dust is composed simply of tiny jagged fragments. For the high temperature Al_2O_3 tests, however, even at $\dot{\varepsilon} = 10^3 s^{-1}$ the dust consists of individual, perfect crystallites of sapphire, as shown in the SEM micrograph of Figure 3.

An interesting feature is revealed upon inspecting at high magnification the intergranular facets for T>1000°C. Regardless of the imposed loading rate, each facet is covered with what seems to be the remains of a liquid phase which has agglomerated into solidified globules (Figure 4a). It should be emphasized that these globules are not fracture debris; each compressive fracture fragment was immersed in alcohol and cleaned ultrasonically prior to coating for SEM study. This process, for tests at T<1000°C, produces intergranular facets which are perfectly devoid of such globules (see Figure 4b, an intergranular facet produced by compressive failure at $\dot{\varepsilon} = 7 \times 10^{-5} s^{-1}$, T = 600°C).

The mapping of σ_c (T, $\dot{\varepsilon}$) for SiC is not yet complete, with lower strain rate, elevated temperature tests still to be run, as indicated in Figure 5. However, certain interesting facts already are apparent. For example, as for the Al_2O_3, an increase in strength with temperature (up to ~700°C) is experienced during rapid loading. This is not the usual trend found for metals; although the strength is usually greatest, for a given temperature, at the highest strain rate, at best the strength is generally only approximately constant at low and intermediate temperatures before decreasing at elevated temperature.

At ~1600°C, the SiC compressive strength at $\dot{\varepsilon} = 2 \times 10^3 s^{-1}$ has decreased relative to that at room temperature by only some 14%, while for Al_2O_3, the observed decrease under the same conditions was ~38%. This relative insensitivity of high $\dot{\varepsilon}$ SiC fracture strength to elevated temperatures is reflected in its fractography, shown in Figure 6. This transgranular failure mode is identical to that reported[5] for lower temperatures and strain rates, as indicated in Figure 5. Within the low $\dot{\varepsilon}$, high T region (question mark inside the dashed zone) intergranular failure may occur; tests are in progress to establish this point, as well as the acoustic emission-determined microcrack nucleation threshold for T>600°C.

Compressive testing of Si_3N_4 is currently underway, and only initial high temperature, high strain data are available. For T = 1675°C and $\dot{\varepsilon} = 2 \times 10^3 s^{-1}$, the compressive strength is 1990 MNm^{-2}, approximately half the corresponding value for SiC (4000 MNm^{-2}).

B. Elevated Temperature Indentation Tests

Hot hardness results for Al_2O_3 are shown in Figure 7 to 1000°C. A peak is observed in the data at T≈325°C, interrupting an otherwise generally decreasing hardness trend with increasing temperature. It will be recalled that a transition in compressive strength with temperature

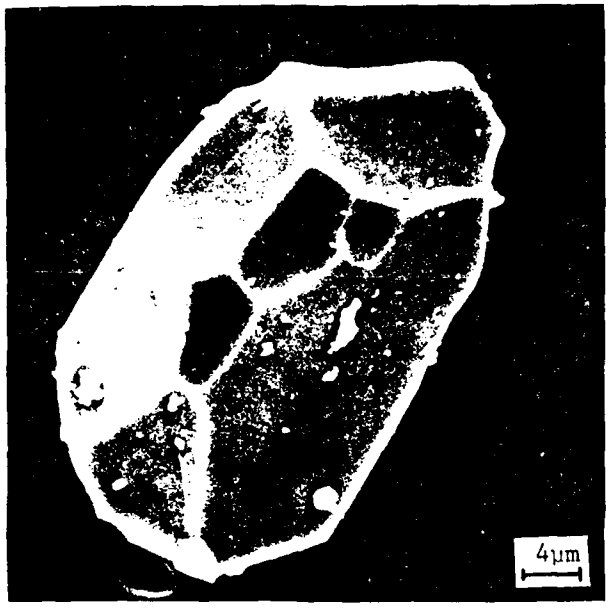

Figure 3. Particulate (Crystallite) Remnant of Al_2O_3 Compressive Failure, $\dot{\varepsilon} = 2 \times 10^{3} s^{-1}$, T = 1500°C.

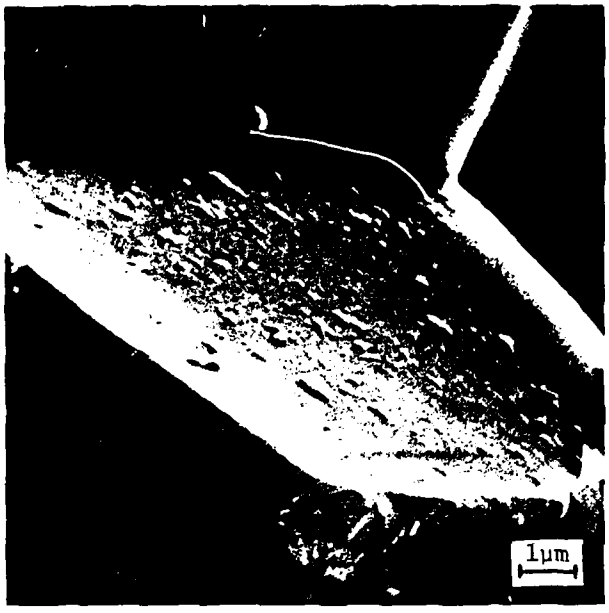

a) Globular Glassy Phase, $\dot{\epsilon} = 2 \times 10^{3} s^{-1}$, T = 1500°C

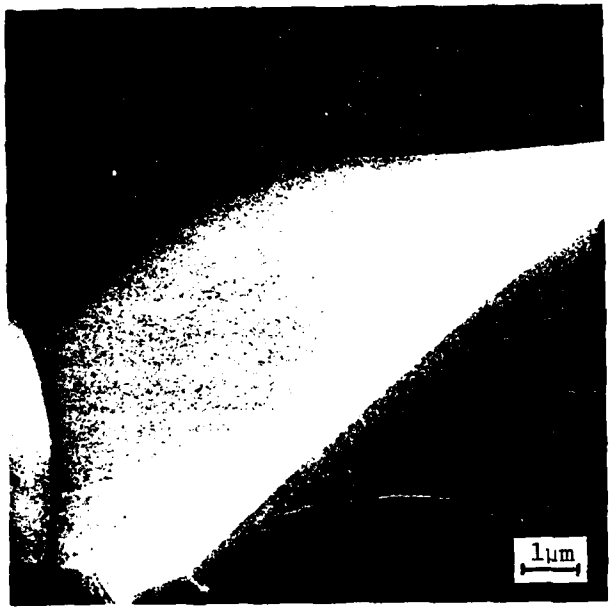

b) Smooth Facet, $\dot{\epsilon} = 7 \times 10^{-5} s^{-1}$, T = 600°C

Figure 4. Al_2O_3 Intergranular Facets Attending Compressive Failure.

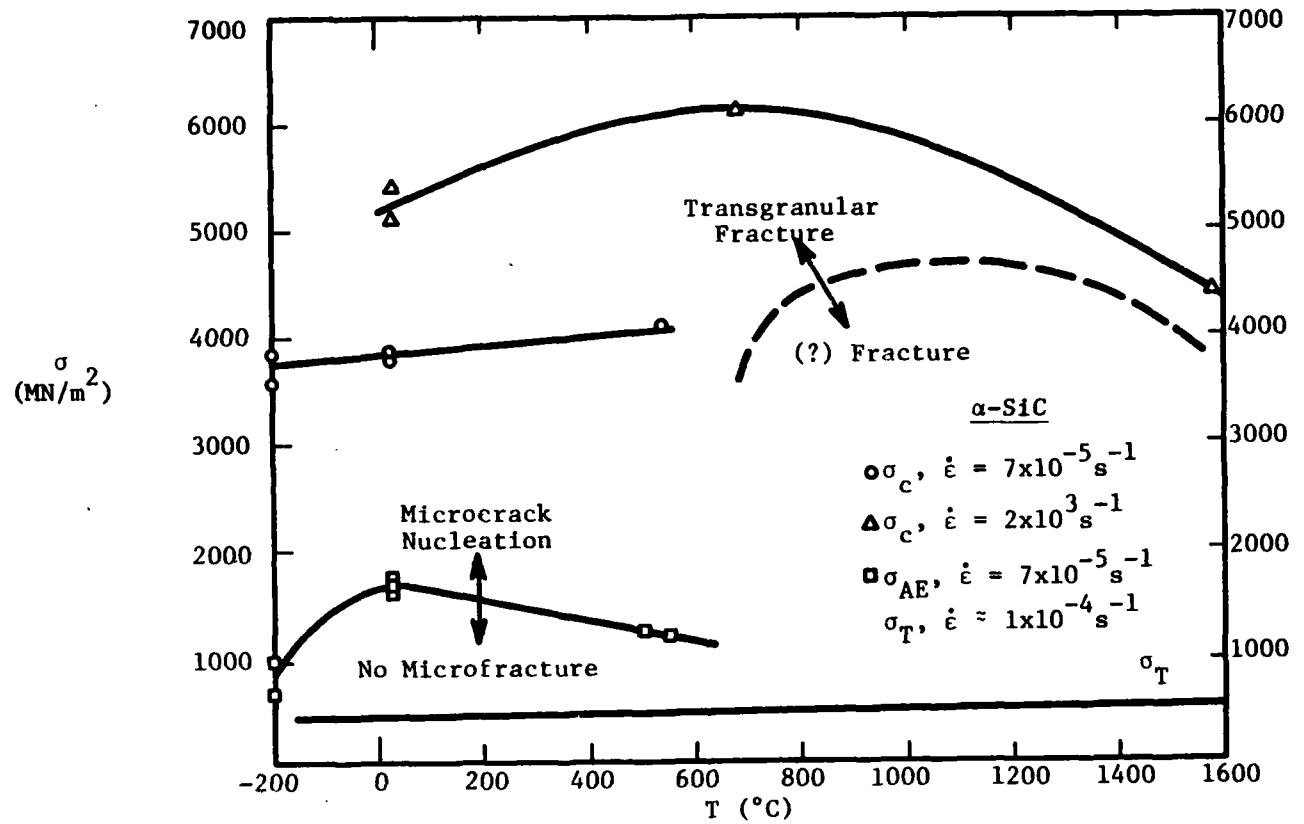

Figure 5. SiC Strength Versus Temperature and Strain Rate.

Figure 6. Transgranular SiC Compressive Fracture Surface, $\dot{\varepsilon} = 2 \times 10^{3} s^{-1}$, T = 1575°C.

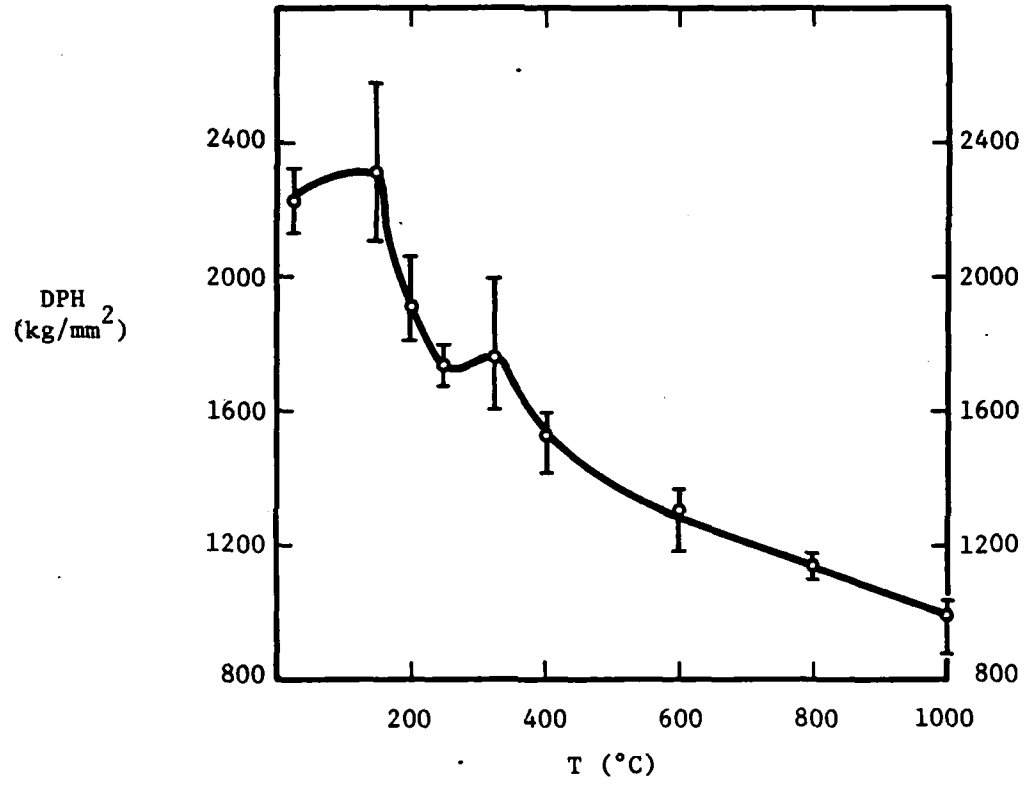

Figure 7. Hardness Versus Temperature for Al_2O_3.

also was observed at approximately the same temperature for the lower strain rates.

Indentation fracture behavior typical of the temperature extremes covered in the indentation tests is seen in Figure 8. At 23°C, fracture is transgranular, both for lateral and radial microcracking (Figure 8a). In contrast, microfracture at 1000°C, under identical loading conditions, is predominantly intergranular (Figure 8b). The relationship of radial cracking to grain boundaries is evident, as is the loss of material caused by lateral cracking along grain boundaries.

Similar hot hardness results are shown in Figure 9 for SiC and Si_3N_4 (indentation fracture analysis is not yet complete). The SiC data exhibit a plateau of constant hardness from 23° to 400°C; a similar effect has been reported by Naylor and Page[8] for SiC. The hardness of Si_3N_4, on the other hand, drops off continuously with increasing temperature. It is notable that over the temperature range studied, the relative decrease in hardness is much less for Si_3N_4 than for either Al_2O_3 or SiC.

IV. Discussion

It is clear that compressive failure in Al_2O_3 is extremely sensitive to loading rate and temperature, and that this failure sensitivity has underlying causes reflected in its fractography. These same failure modes seem to manifest themselves during indentation fracture, as well, at corresponding temperatures. The observed high temperature liquid phase globules are probably composed of spinel ($MgAl_2O_4$), based on scanning Auger microprobe work by Johnson.[9] It is intriguing that high temperature intergranular failure persists at high loading rates, since the viscous decohesion process might be expected to be somewhat slower than transgranular cleavage; apparently, this is not the case.

It is possible to combine the compressive strength and hardness results in an interesting way to assess the possible roles which they may play in indentation fracture. Already it is clear that the two parameters are intimately related, as previously suggested by Rice,[1] both decreasing with increasing temperature in a relatively proportional fashion, and experiencing some sort of transition at T~350°C.

Lawn and Evans[2] have modelled the threshold microfracture process for indentation at sharp indenters, finding that the threshold crack size C^* should be proportional to $(\frac{K_c}{H})^2$, where K_c is the fracture toughness. Using the present low loading rate H(T) data, since the indentations were created quasistatically, and $K_c(T)$ results of others,[10] it is possible to plot $C^*/C_o(T)$, where C_o is the threshold indentation radial crack size under room temperature, quasistatic loading, as shown in Figure 10. It is evident that this relation does not predict the observed results very well over the temperature range studied. However, if σ_c is used

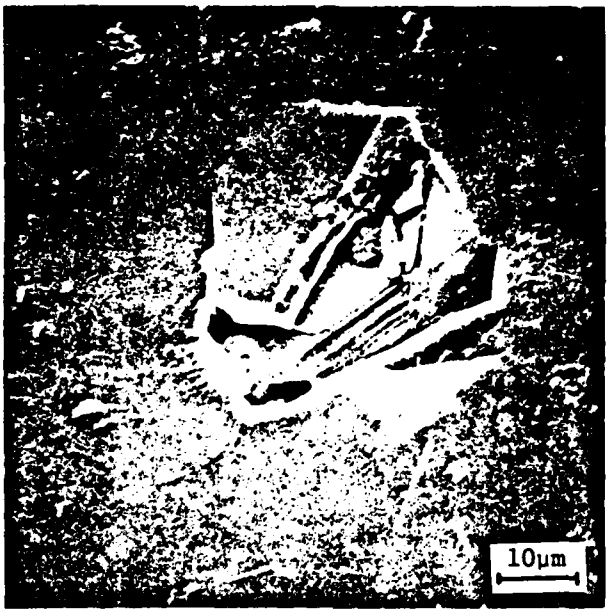

a) Transgranular Microfracture, T = 23°C

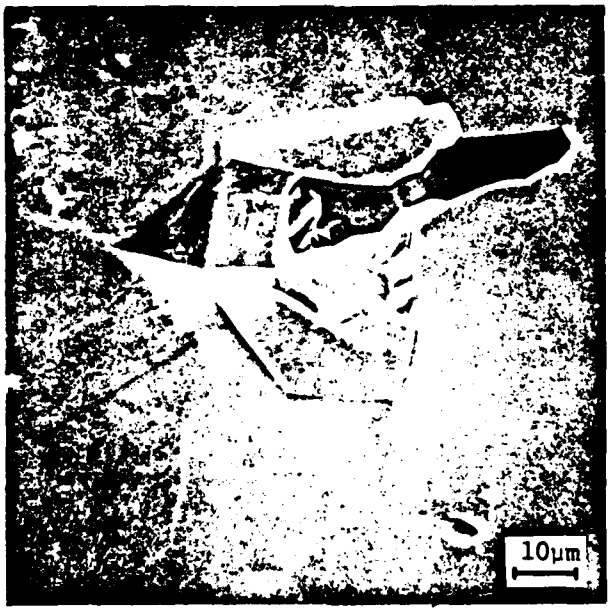

b) Intergranular Microfracture, T = 1000°C

Figure 8. Indentation Fracture, Al_2O_3, Load = 600 gm.

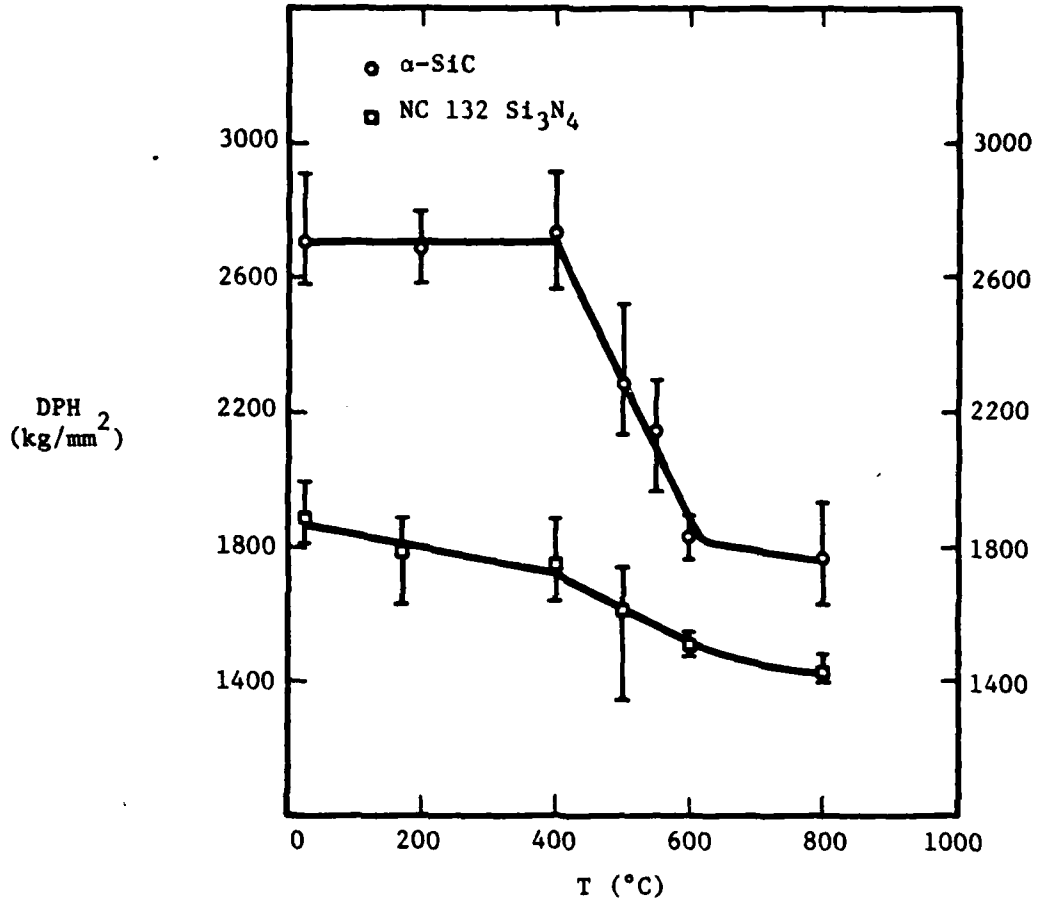

Figure 9. Hardness Versus Temperature for SiC and Si_3N_4.

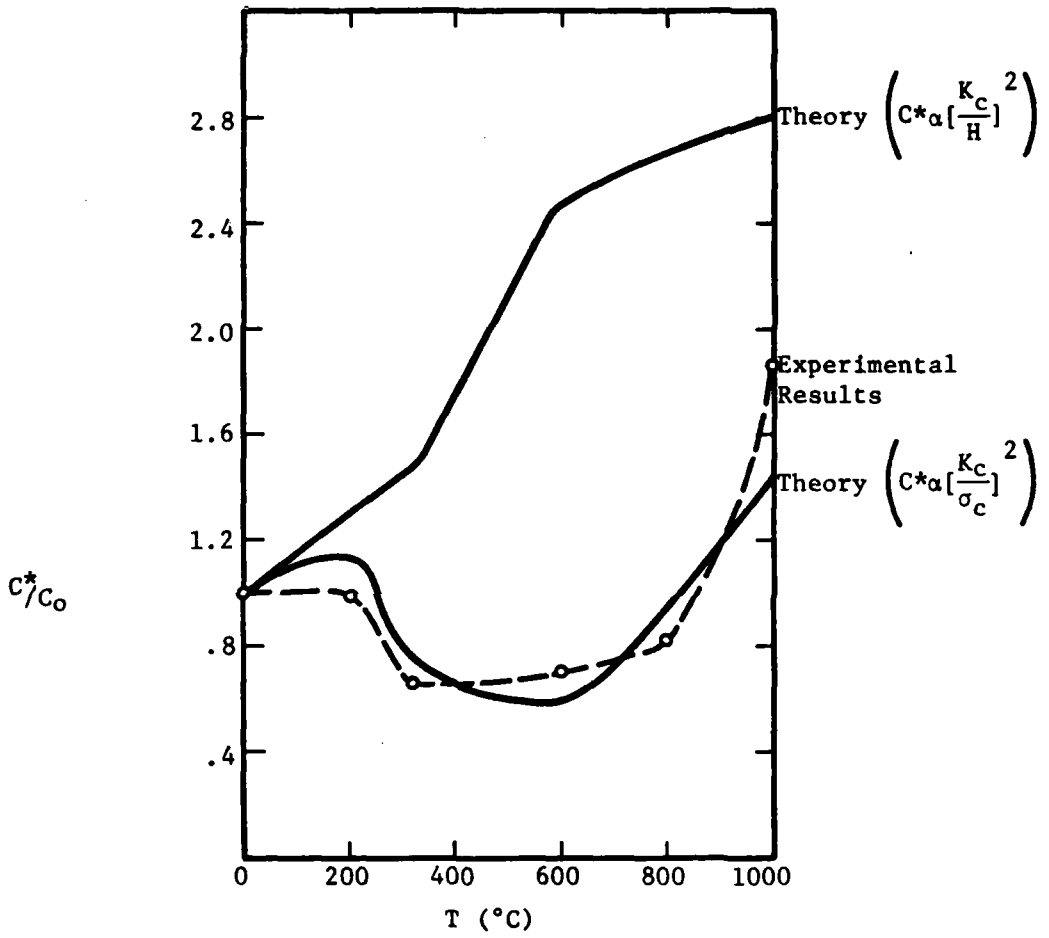

Figure 10. Threshold Indentation Crack Size Versus Temperature for Al_2O_3.

for H instead (in effect assuming that an indentation test for a brittle material is a microcompression test), the results are predicted quite faithfully. Thus, both the indentation crack size relationship and the mode of indentation fracture in Al_2O_3 are predicted by compression test results.

The picture is not yet complete for SiC and Si_3N_4, but some observations can be made. For example, as noted, the lack of temperature sensitivity for the high $\dot{\varepsilon}$ compression tests is reflected in the fractography, i.e., non-intergranular. This is reasonable, since it is thought that the grain boundaries in sintered α-SiC are essentially free of second phase microconstituents. Whatever propensity the material might exhibit for intergranular separation at lower $\dot{\varepsilon}$ is defeated by strain rates $\geq 10^3 s^{-1}$.

From 23° to 550°C, the compressive strength of SiC at low temperature is basically flat, qualitatively mirroring the observed hardness plateau to 400°C. It is expected that $\sigma_c(T)$ should then begin to decrease if σ_c and H are related; this seems likely, based on the high rate data which begins to drop off at T~650°C. Indentation cracking observations are incomplete at present, so that fracture modes and C* are unavailable.

For NC-132 Si_3N_4, however, threshold crack size data were obtained, and can be plotted as in Figure 11. In this case, the experimental data correlate very well with $C^* \alpha (\frac{K_c}{H})^2$ until T>600°C, when a divergent result is obtained; this time the theory seems to underestimate the threshold crack size. However, these results are not conclusive, and await comparison with predictions based on $(\frac{K_c}{\sigma_c})^2$; such comparison will be possible upon completion of the lower strain rate $\sigma_c(T)$ compression tests.

In conclusion, the following observations are made:

(1) Indentation microfracture seems to reflect compressive microfracture mode at corresponding temperature and loading rate.

(2) $\sigma_c(T)$ and H(T) behave in qualitatively similar fashion.

(3) It is possible that $\sigma_c(T)$ is at least as valid as H(T) in predicting indentation cracking threshold parameters.

(4) Based on $\sigma_c(T)$ data, it would be expected that under impact indentation conditions, the indentation cracking threshold would be greatly modified over that predicted by quasistatic H(T) measurements.

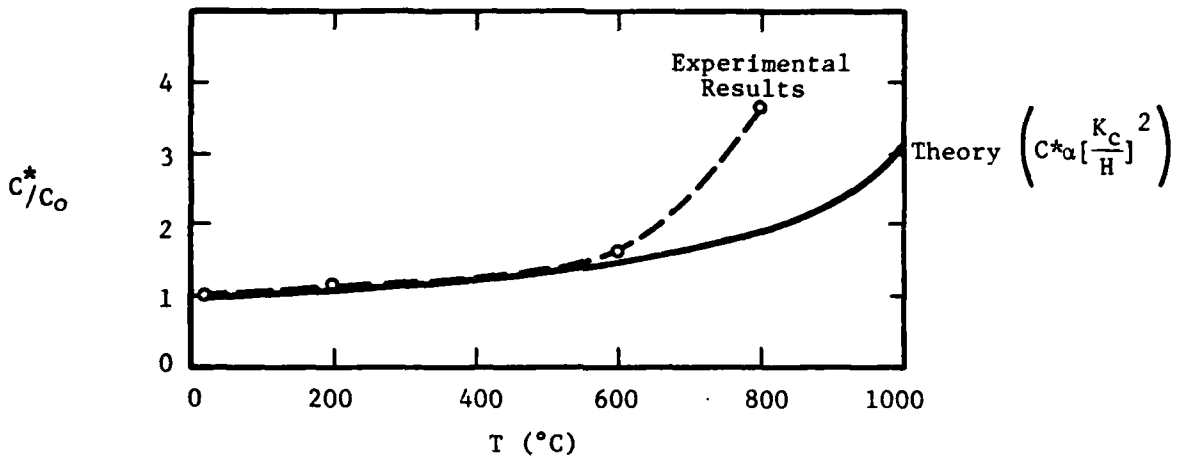

Figure 11. Threshold Indentation Crack Size Versus Temperature for Si_3N_4.

V. Acknowledgements

The author is very grateful to H. Muehlenhaupt for his excellent, careful work in carrying out the difficult high loading rate, high temperature compression tests, to M. Luckey for precision grinding the compression specimens and platens, and to A. Nicholls for his meticulous job of carrying out the tedious elevated temperature indentation tests.

VI. References

1. R. W. Rice, Mat. Sci. Res., 5, ed. W. W. Kriegel, Plenum Press, N. Y., 1970, 195.

2. B. R. Lawn and A. G. Evans, Jour. Mat. Sci., 12, 1977, 2195.

3. J. Lankford and D. L. Davidson, Jour. Mat. Sci., 14, 1979, 1662.

4. J. Lankford, Jour. Mat. Sci., 12, 1977, 791.

5. J. Lankford, Jour. Am. Cer. Soc., 62, 1979, 310.

6. J. Lankford, Fracture Mechanics of Ceramics, ed. R. C. Bradt, D. P. H. Hasselman, and F. F. Lange, Plenum Press, N.Y., 1978, 245.

7. J. Lankford and D. L. Davidson, "Compressive Strength and Indentation Damage in Ceramic Materials," ONR Technical Report, Contract No. N00014-75-C-0668, May, 1978.

8. M. G. S. Naylor and T. F. Page, Proc. 5th Int. Conf. Erosion by Solid and Liq. Impact, Cambridge Univ. Press, 1979, 32-1.

9. W. C. Johnson, Jour. Am. Cer. Soc., 61, 1978, 234.

10. A. G. Evans, M. Linzer, and L. R. Russell, Mat. Sci. Eng., 15, 1974, 253.